5.3 Publicación 3

Titanium (IV) oxide thin films obtained by a two-step soft-solution method

Ana M. Peiró,[a] Elena Vigil,[b] José Peral,[a] Concepción Domingo,[c] Xavier Domènech[a] and José A. Ayllón[a]

[a] Departament de Química, Universitat Autònoma de Barcelona, 08193 Bellaterra, Barcelona, Spain

[b] Facultad de Física - Instituto de Materiales y Reactivos (IMRE), Universidad de La Habana, Colina Universitaria, Ciudad Habana, Cuba

[b] Institut de Ciència de Materials de Barcelona (CSIC), Campus de la UAB, 08193 Bellaterra, Barcelona, Spain

Thin Solid Films 411 (2002) 185-191

ELSEVIER

Thin Solid Films 411 (2002) 185–191

thin solid films

www.elsevier.com/locate/tsf

Titanium(IV) oxide thin films obtained by a two-step soft-solution method

Ana M. Peiró[a], Elena Vigil[b], José Peral[a], Concepción Domingo[c], Xavier Domènech[a], José A. Ayllón[a,*]

[a]*Departament de Química, Universitat Autònoma de Barcelona, 08193 Bellaterra, Spain*
[b]*Universidad de La Habana, Facultad de Física–Instituto de Materiales y Reactivos (IMRE), Universidad de La Habana, Colina Universitaria, Ciudad Habana, Cuba*
[c]*Institut de Ciència de Materials de Barcelona, CSIC, 08193 Bellaterra, Spain*

Received 20 July 2001; received in revised form 20 March 2002; accepted 20 March 2002

Abstract

TiO_2 films were deposited on either glass or Si substrates by using a two-step soft-solution method. A submonolayer of anatase TiO_2 nanocrystals was first deposited on the substrate by a drain-coating process that was performed at 333 K from an aqueous TiO_2 colloidal solution. The substrate partially covered with the TiO_2 nanocrystals was immersed in an aqueous solution, containing a titania precursor [fluorine-complexed Ti(IV)], and the whole was treated with microwave irradiation. The nanocrystals deposited on the substrate acted as growth seeds in the subsequent formation of the TiO_2 film. The obtained TiO_2 films showed a high degree of crystallinity (anatase), even without further thermal treatment; however, they did not show photocatalytic activity. Thickness of the films was varied as a function of microwave power and irradiation time.

Keywords: Titanium oxide; Deposition process; Microwave; Soft-solution processing

1. Introduction

Titanium dioxide (TiO_2) films find extensive application in several fields such as photocatalysis [1,2], dye sensitized solar cells [3,4] or anti-reflectance coatings [5,6]. To prepare the films, dry methods [i.e. chemical vapor deposition (CVD) [7,8], sputtering [9], etc.] and wet methods [sol–gel [2], Langmuir–Blodgett films [10], self-assembled monolayers [11–13], liquid phase deposition (LPD) [14–17]] are employed. The wet methods usually require a thermal post-treatment in order to eliminate organics present in the films or to induce crystallization of the deposited material. Sometimes, post-annealing is also required for films obtained by dry methods.

Methods for the preparation of crystalline TiO_2 films at low temperatures, with low-cost equipment and using water as a solvent are not extensively found in the literature [18]. The development of 'soft-solution processing' methods for the formation of advanced inorganic materials, such as oxide films, is nowadays gaining much attention [19]. Simple equipment and low energy requirement are the main characteristics of these methods. Hydrothermal [20] and electrochemical [20,21] processes are examples of soft methodologies, as they allow the formation of crystalline films 'in situ', without the need of an annealing post-treatment. In addition, the use of aqueous solutions instead of organic solvents is desirable for environmental and economic reasons.

Recently, two methods for the preparation of TiO_2 films have been developed in our laboratory [22–25], in which crystalline films of anatase are obtained with relative ease under mild conditions, i.e. ambient pressure and temperature not higher than 373 K. No further thermal treatment is required in either method.

The first method deals with the deposition of thin films of TiO_2 on glass substrates with one-side covered by a transparent conductive oxide. Microwave (MW)

*Corresponding author. Departament de Química, Universitat Autònoma de Barcelona, Edificio Cn, Campus de la UAB, 08193 Bellaterra, Spain. Tel.: +34-93-581-29-19; fax: +34-93-581-29-20.
E-mail address: joseantonio.ayllon@uab.es (J.A. Ayllón).

0040-6090/02/$ - see front matter
PII: S0040-6090(02)00276-6

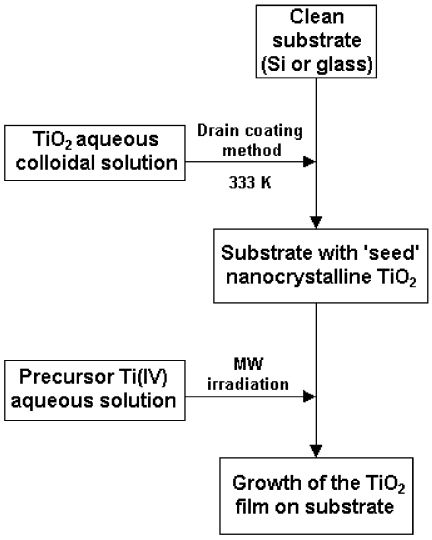

Fig. 1. Flow chart showing the preparation process of TiO_2 films.

irradiation was supplied to promote oxide formation from homogeneous aqueous solutions of different precursors [22–24]. Characterization of the films reveals that they consist of crystals with linear dimensions under 100 nm forming a compact, well-adhered and homogeneous film of TiO_2. Well-adhered TiO_2 films do not grow on the uncovered side of the glass. It is argued that nucleation of TiO_2 crystallites on the conducting surface is enhanced by the interaction of microwave radiation with the electrons already present in this surface. The possible role of the substrate acting as a seed for nucleation is also mentioned.

The second method consists in the deposition of TiO_2 films on several substrates (glass, F-doped SnO_2 covered glass or silicon wafer) by a drain-coating method from an aqueous solution of colloidal anatase [25]. The process is performed in an open atmosphere at the low temperature of 333 K. The colloidal TiO_2 obtained under mild conditions comprises anatase nanoparticles of approximately 9×5-nm size, stabilized by tetrabutylammonium cations (TBA^+). The obtained titania films are very thin, transparent and show good adherence. Different film thickness can be obtained by consecutive deposition processes.

In this paper, thin films of TiO_2 are deposited on either glass or (100)-oriented silicon (Si) substrate by a combination of the two procedures described above (Fig. 1). According to previous results, it seems reasonable to assume that the growth of TiO_2 films by using the first method is favored when adequate nucleation sites are already present on the substrate surface. The deposition of TiO_2 anatase nanocrystal seeds (the nucleation sites) is attained by using the second method.

2. Experimental

2.1. Substrates cleaning previous to deposition process

Substrates were cleaned just before performing the deposition process. Glass slides (Knittel Gläser, Germany) were succesively immersed for 30 min in boiling sulfuric acid and Milli-Q water (Millipore), followed by 5-min ultrasonic cleaning in acetone (analytical grade, Merck) and absolute ethanol (EtOH, analytical grade, Panreac). Finally, they were rinsed with water. The organic contaminants of the (100)-oriented Si substrates were removed by sequential 5-min ultrasonication in acetone and EtOH, followed by a water rinse. In order to eliminate the formed superficial layer of silicon oxide from the surface, the Si substrates were immersed in diluted hydrofluoric acid (HF, analytical grade, 40%, Fluka) for a few seconds and thoroughly rinsed with water afterwards.

2.2. Preparation of the TiO_2 aqueous colloidal solution

The TiO_2 aqueous colloidal solution was freshly prepared as described elsewhere [25,26]. Briefly, 5 ml of titanium tetraisopropoxide (TIP, technical grade, Fluka) were dissolved in 30 ml of abs. EtOH. The mixture was then added to a solution of 0.6 ml tetrabutylammonium hydroxide (TBAOH, 40%, purum, Fluka) and 30 ml EtOH. Solutions were protected from atmosphere moisture before being mixed. Afterwards, 185 ml of water was added. The obtained transparent solution, with a final Ti:TBA 19:1 mole ratio, was heated to evaporate the ethanol and 2-propanol (a TIP hydrolysis by-product) until the volume of the solution was reduced to approximately 100 ml. This solution was heated to reflux for 2 h using a MW furnace (Prolabo Maxidigest MX350) working at 60 W. The obtained colloidal TiO_2 solution was fivefold diluted with water prior to its use.

2.3. Pre-treatment of the substrates using the drain-coating method

For the deposition of 'seed' anatase nanocrystals, the drain-coating method was employed. Substrates were immersed for 5 min into 100 ml of the anatase colloidal solution prepared according to Section 2.2, which was maintained at 333 K in a thermostated vessel. Afterwards, the solution level was lowered at the rate of 23 mm/min by means of a peristaltic pump connected to an open end in the bottom of the vessel. Upon removal from the solution, the substrates were carefully rinsed with water and dried under a N_2 stream.

2.4. Preparation of the precursor fluorine complexed Ti(IV) aqueous solution

The aqueous solution of the Ti(IV) precursor was freshly prepared as described in Vigil et al. [23] with

minor modifications. A fluorine-complexed titanium(IV) solution was made in a plastic vessel by preparing first a solution constituted of 10 ml of TIP (0.034 mol) and 50 ml of EtOH, and adding then 6 ml of an aqueous solution of HF (0.136 mol). Solutions were ice-cooled before being mixed. Afterwards, 100 ml of an aqueous solution of ammonium fluoride (NH_4F, analytical grade, Fluka) (0.068 mol) was added. The obtained clear solution was heated in an open vessel in order to evaporate the alcohols, until the volume was reduced to approximately 70 ml. The obtained residue was diluted up to 1 l with water. The precursor was formed after mixing equal volumes of the Ti(IV) solution ($[Ti]=3.4\times10^{-2}$ M) and a boric acid (analytical grade, Fluka) solution (6.8×10^{-2} M). The pH was adjusted at 2.4 with hydrochloric acid (analytical grade, 25%, Fluka).

2.5. Growth of TiO_2 films from a microwave-activated solution

Substrates pre-treated as explained in Section 2.3 were immersed in 50 ml of the precursor Ti(IV) solution (Section 2.4). The whole was first ultrasonnicated during 1 min, and, then, MW irradiated. Different MW power and irradiation time combinations were tested. After microwaving, substrates were taken out of the solution and rinsed with water. Before characterization, samples were thoroughly cleaned by sequential 5-min ultrasonnication in acetone and EtOH, rinsed with water and dried under a N_2 stream. The obtained TiO_2 films showed reflection-interference colors (yellow, blue, pink and green) with yellow corresponding to the thinnest films. An abbreviation indicating the nature of the substrate, Si for silicon or G for glass, was used to label the samples, in addition to the values of power and irradiation time, which defined each working regime. For example, a Si-60-5 is a sample obtained using a silicon substrate with a 60-W power applied during 5 min.

2.6. Characterization techniques

Thickness measurements were performed using a scanning electron microscope (SEM, Hitachi S-570 and JEOL JSM-6300). Some of the samples chosen for thickness measurements presented clear steps, which could be seen with the naked eye. The extreme experimental conditions employed in their preparation (long time or high MW power) resulted in film detachment and formation of steps. Other samples were cut into pieces resulting in the break of the TiO_2 film near the cut edge of the substrate. Film thickness was studied in these edges. Samples were gold-covered and mounted onto a sample holder with an inclination of 45° with respect to the electron beam. TiO_2 films were easily distinguished from the bare substrate because of their different roughness. Layer thickness was obtained after dividing the thickness observed in SEM micrographs by the sinus of 45°, in order to take into account the inclination of the sample holder. Surface characteristics of gold-covered films were further investigated by SEM. To study the atom ordering, grazing angle X-ray diffraction (XRD) patterns of the deposited films were recorded using a Siemens D-3400 apparatus, operated at 40 kV and 30 mA. The diffraction spectra were recorded at incidence angles of 0.3 and 0.6° over the range $20<2\theta<65$. CuKα radiation ($\lambda=0.154056$ nm) was used for all X-ray measurements. Fourier transform infrared spectra (FTIR) of TiO_2 films on Si substrates were recorded using a Perkin Elmer 2000 system.

2.7. Photocatalysis experiments

The photoactivity of TiO_2 films on glass slides was evaluated through the analysis of the degradation of salicylic acid under UV-illumination. Experiments were conducted in a cylindrical Pyrex cell of 0.13-l capacity thermostated at 298 K. A 125-W Philips HPK medium pressure mercury vapor lamp was used as the light source. An aqueous solution of salicylic acid (6.25×10^{-5} M, 100 ml) was used. The solution inside the cell was stirred and air was bubbled into it during the experiment. Absorbances of both initial and irradiated samples were determined using a Philips PU 8620 UV/VIS/NIR spectrophotometer at a wavelength of 296 nm, using a quartz cuvette with 4 cm of optical path length.

3. Results and discussion

3.1. Deposition of TiO_2 films: thickness, color and transmittance

The process of deposition of TiO_2 films onto glass and Si substrates is schematically depicted in Fig. 1. The first step was the deposition of anatase nanocrystals by the drain-coating technique. This pre-treatment was performed under mild conditions and in an easy way, since: (i) an aqueous solvent was used; (ii) it was carried out at a low temperature; and (iii) it was performed in an open atmosphere. For all the treated substrates, the working experimental conditions, colloidal solution concentration and temperature, were similar. The amount of TiO_2 deposited in this step was extremely low and was not detectable by the naked eye. Previous studies, based on atomic force microscopy observation, showed that the substrate surface was only partially covered [25]. By repeating the drain coating process several times, a full coverage could be attained and the film thickness was enlarged. However, this was a laborious and time-consuming process, e.g. after 25 process-

Table 1
Characteristics of TiO_2 films grown on Si substrates under different regimes

Sample	Microwave power (W)	Irradiation time (min)	Mean particle diameter (nm)	Reflection-interference color
Si-60-10	60	10	60 ± 10	Yellow with blue pints
Si-60-20	60	10	60 ± 10	Yellow or blue
Si-90-10	90	10	70 ± 15	Yellow or blue
Si-120-5	120	5	60 ± 15	Yellow or blue
Si-120-10	120	10	70 ± 25	Yellow or pink
Si-120-20	120	20	80 ± 25	Yellow with blue pints
Si-150-5	150	5	85 ± 25	Dark and light blue
Si-180-5	180	5	80 ± 30	Yellow or blue

es film thickness was only equivalent to 50 nm of non-porous TiO_2. In the present work, rapid film growth was attained after seed deposition by a second step in which MW irradiation was applied to the substrate immersed in an aqueous solution of Ti(IV) fluorine complex as the titania precursor.

Table 1 shows the characteristics of TiO_2 films grown on Si substrates at different MW power and irradiation times. A proper combination of both experimental parameters yielded well-adhered films, which were transparent and colored by the interference of light. In general, a short irradiation or heating time required a high microwave power; no deposition was observed for low power and short irradiation time (e.g. regimes: Si-30-5, Si-60-5 and Si-90-5). On the other hand, for a long time or high irradiation power (e.g. regimes: Si-60-30, Si-90-20 and Si-150-20), partial detachment of the TiO_2 layer was observed. TiO_2 films were also deposited on glass substrates at different regimes, applying similar experimental conditions to those used for deposition on Si. In this case, a smaller range of MW power and time could be used to obtain a non-scratched film. It was observed that low microwave power and long deposition time yielded thick films; e.g. the sample obtained with a regime G-30-30, showed a green color due to the interference of light (see Table 2 for the dependence between the color of the layer and the thickness). However, the obtained thick film was partially detached. This problem could be overcome combining high microwave power with short deposition time. Thin films could then be thickened by consecutive deposition processes. For example, regime G-210-3 yielded samples with a faint yellow color which resulted in a yellow layer after treating the sample under similar conditions for a second time. Thicker layers, between 50 and 400 nm (blue, green or pink colored), were obtained by performing consecutive deposition processes. Deposition rates varied from 5 to 15 nm/min depending on the experimental conditions.

Table 2
Thickness range of TiO_2 films grown on glass and Si substrates under different regimes, and dependence on their reflection-interference colors

Reflection-interference color	Thickness range (nm)	
	Glass substrate	Si (100) substrate
Light yellow	150–180	<140
Yellow	180–240	<140
Light blue	240–270	140–180
Pink	300–360	300–360
Green	480–540	390–450

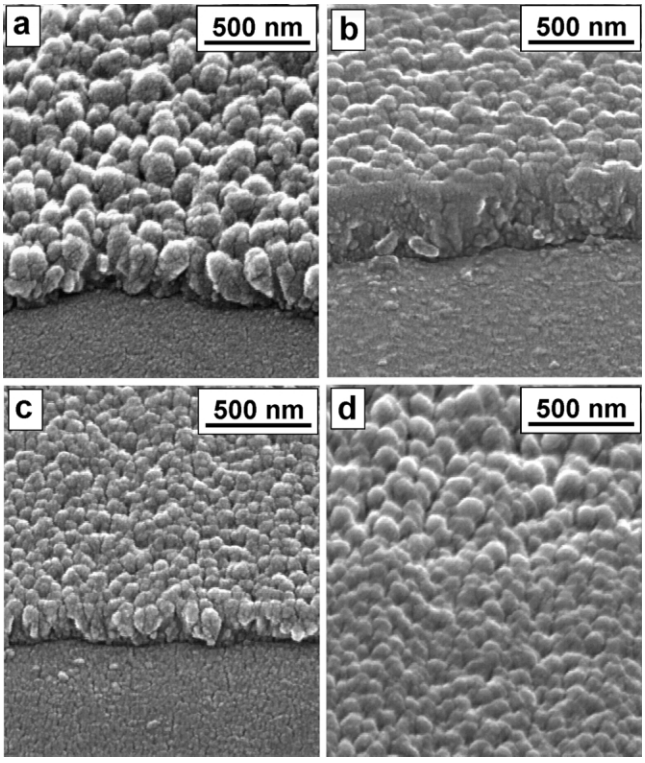

Fig. 2. Cross-section SEM micrographs of TiO_2 films obtained on Si and glass substrates under different regimes: (a) Si-60-20, (b) G-30-60, (c) G-150-11 and (d) Si-60-15.

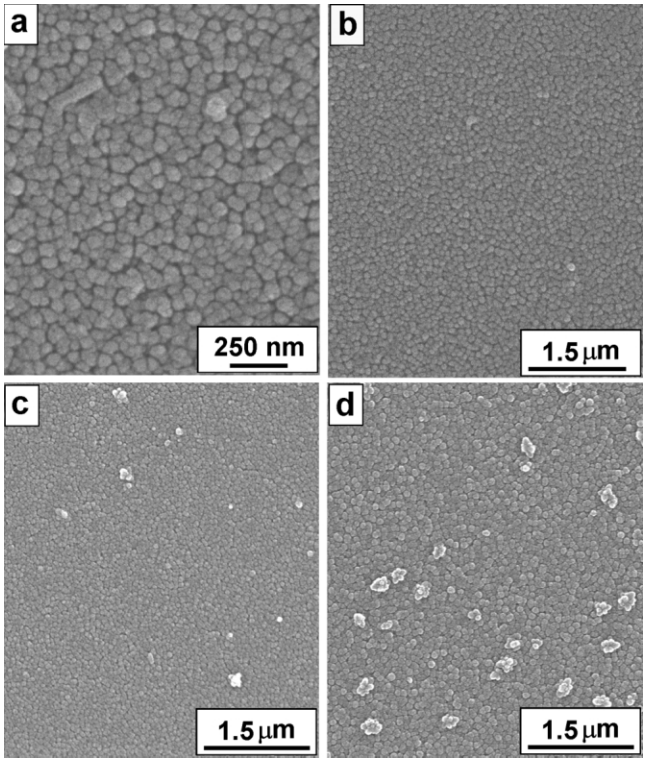

Fig. 3. SEM micrographs of the surface of TiO_2 films deposited on glass and Si substrates under different regimes: (a,b) G-60-20 observed at different magnification orders, (c) Si-120-5, and (d) Si-150-5.

Fig. 2 shows cross-section SEM micrographs of TiO_2 films grown on glass and Si substrates. For films having the same color in both substrates, larger grains with a better shape definition were observed on Si substrates when compared to glass substrates (Fig. 2a,b, respectively). It was also observed that grain dimensions in the thinner layers were smaller than in the thicker ones (see Fig. 2a,c for TiO_2 grown on Si substrate). Table 2 shows the correlation between the film thickness and the interference color for layers grown on glass and Si substrates. This dependence was in accordance with data reported by Vigil et al. [23] for TiO_2 layers deposited on indium tin oxide (ITO) conducting glass. Fig. 2d shows the surface of a sample in which two different layer thicknesses meet together. Larger grains were found on the top (pink layer) than on the bottom (thin yellow layer). This fact further confirms the mentioned dependence between film thickness and grain size.

3.2. Scanning electron micrographs of TiO_2 films

Surface characteristics of TiO_2 films deposited on glass and Si substrates were also studied by SEM (Fig. 3). A similar layer morphology was obtained regardless of the substrate employed. SEM analysis showed that films consisted of crystals with linear dimensions under 100 nm forming a compact layer. Moreover, no intragranular porosity, beyond the detection limit, could be observed, neither in cross-section nor in surface micrographs. The size of the crystallites was dependent on the irradiation time and MW power, as shown in Table 1. The mean grain size value increased when raising the MW power from 60 to 85 W, but, unfortunately, also the grain size distribution broadened (compare Fig. 3c,d). Also, a large number of loose adhered flower-like TiO_2 crystals were observed on the film surface for high MW powers. These deposits gave the films a whitish appearance as they strongly scattered light. After ultrasonnication, which removed most of these deposits, a very well adhered colored transparent film was obtained. These films had similar characteristics to those grown on conducting glass using a similar fluorine-complexed Ti(IV) precursor solution and applying microwave irradiation at different regimes [23].

3.3. X-Ray diffraction studies

Fig. 4 shows the recorded XRD patterns of a TiO_2 film deposited on a glass substrate at different stages. The peak assignments are indicated next to the respective Bragg reflections. Trace (a) corresponds to the spectrum obtained for the substrate after performing the drain-coating pre-treatment; and trace (b) after the complete two-step process (regime G-60-20). In trace (a) no relevant signals were observed, likely due to the low amount of TiO_2 deposited in the drain-coating step. In trace (b) reflections for TiO_2 films were sharp and clearly showed the presence of the anatase structure. The peak intensities differ from those of the anatase

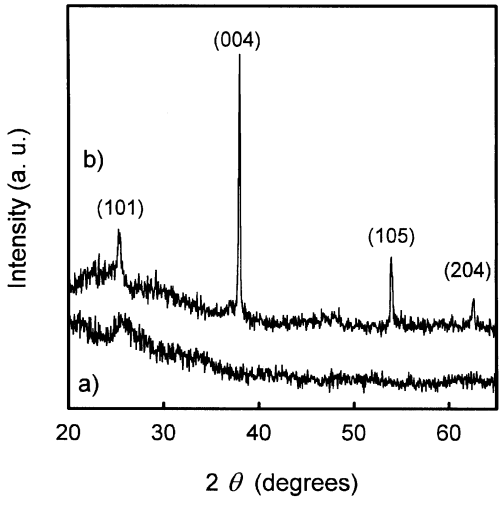

Fig. 4. X-Ray diffraction spectra corresponding to a glass substrate: (a) after the drain-coating pre-treatment, and (b) after the second step carried out under regime G-60-20. The peak assignments are indicated next to the respective Bragg reflections.

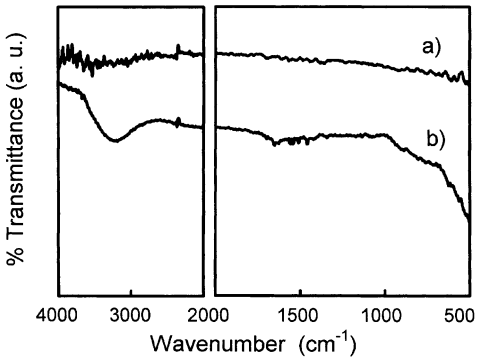

Fig. 5. FTIR spectra corresponding to a Si substrate: (a) after the drain-coating pre-treatment, and (b) after the second step carried out under regime Si-60-20.

patron (which correspond to complete random order). For example the relative intensity of the peak corresponding to the (004) plane at 37.8° was notably increased, while that of (112) plane at 38.6° was very weak. This preferential growth and high crystallinity could be attributed to the presence of fluoride anion [27].

3.4. FTIR studies

Fig. 5 shows the FTIR spectra of a TiO_2 film grown on a Si substrate at different stages. Fig. 5a corresponds to the spectrum obtained for the substrate after performing the drain-coating pre-treatment, and Fig. 5b after the complete two-step process (regime Si-60-20). In Fig. 5a no relevant signals were observed, likely due to the low amount of TiO_2 deposited in the drain-coating step. In Fig. 5b the presence of TiO_2 was clearly noted by the absorbance region below 800 cm^{-1} [28,29]. The broad band at 3400 cm^{-1} is characteristic of associated hydroxyl groups. The absence of bands assigned to C–H bonds showed that the TiO_2 film was mainly free of organic moieties from starting products.

3.5. Photocatalysis

No photocatalytic activity was found for salicylic acid degradation under UV-illumination when using these TiO_2 films. This lack of photoactivity was associated to contamination of TiO_2 with fluoride from the precursor used in the second step [29]. It has been reported that fluoride anion competes with organic substances for adsorption on the TiO_2 surface [29–31]. Nevertheless, it has also been reported that the addition of fluoride anions, in proper concentrations, enhances the photocatalytic activity of TiO_2 towards the decomposition of phenol in aqueous solution [32]. The lack of photoactivity could also be ascribed to fluoride anions incorporated in the anatase lattice, i.e. in the bulk of the material [29].

4. Conclusions

Compact layers of anatase TiO_2 with grain sizes between 50 and 100 nm were deposited on Si and glass substrates by a two-step solution process performed at temperatures lower than 373 K. The layers were transparent and colored by reflection-interference of light. The employed deposition method was developed from the combination of two different processes previously reported: deposition from a colloidal aqueous solution and deposition from a soluble precursor induced by microwave radiation. The present two-step process widens the range of substrates in which TiO_2 deposition can be performed using a microwave method. The developed soft-solution method provides a low-cost route to synthesize dense and well-crystallized titanium dioxide films for different applications without any annealing post-treatment being required. The obtained films lack of photocatalytic activity, which could be advantageous for optical or insulating applications.

Acknowledgments

This work was financed by the AMB-12R-CO3-01 CICYT project of the Spanish National Plan of Research. The authors want to thank Dr Puigdollers and Dr Francisco Javier Muñoz for kindly providing Si substrates, and Dr Joan Sola to facilitate use of FT-IR apparatus.

References

[1] J.A. Byrne, B.R. Eggins, N.M.D. Brown, B. McKinney, M. Rouse, Appl. Catal. B: Environ. 17 (1998) 25.
[2] J. Yu, X. Zhao, Q. Zhao, Thin Solid Films 379 (2000) 7.
[3] B. van der Zanden, A. Goossens, J. Phys. Chem. B 104 (2000) 7171.
[4] Y. Li, J. Hagen, W. Schaffrath, P. Otschik, D. Haarer, Sol. Energy Mater. Sol. Cells 56 (1999) 167.
[5] L.M. Doeswijk, H.H.C. de Moor, D.H.A. Blank, H. Rogalla, Appl. Phys. A 69 (Suppl.) (1999) S409.
[6] C. Martinet, V. Paillard, A. Gagnaire, J. Joseph, J. Non-Cryst. Solids 216 (1997) 77.
[7] W.G. Lee, S.J. Woo, J.C. Kim, S.H. Choi, K.H. Oh, Thin Solid Films 237 (1994) 105.
[8] M. Schvisky, A. Harsta, A. Aidla, K. Kukli, A.-A. Kiisler, J. Aarik, J. Electrochem. Soc. 147 (2000) 3319.
[9] D. Mardare, M. Tasca, M. Delibas, G.I. Rusu, Appl. Surf. Sci. 156 (2000) 200.
[10] J. Jin, L.S. Li, Y. Li, X. Chen, L. Jiang, Y.Y. Zhao, T.-T. Li, Thin Solid Films 379 (2000) 218.
[11] H. Shin, R.J. Collins, M.R. De Guire, A.H. Heuer, C.N. Sukenik, J. Mater. Res. 10 (1995) 692.
[12] H. Lin, H. Kozuka, T. Yoko, Thin Solid Films 315 (1998) 111.
[13] Z. Xiao, J. Gu, D. Huang, Z. Lu, Y. Wei, Appl. Surf. Sci. 125 (1998) 85.
[14] K. Shimizu, H. Imai, H. Hirashima, K. Tsukuma, Thin Solid Films 351 (1999) 220.
[15] H. Koshimoto, K. Takahama, N. Hashimoto, Y. Aoi, S. Deki, J. Mater. Chem. 8 (1998) 2019.

[16] S. Deki, Y. Aoi, O. Hiroi, A. Kajinami, Chem. Lett. (1996) 433.
[17] M.-K. Lee, B.-H. Lei, Jpn. J. Appl. Phys. 39 (2000) L101.
[18] H. Lin, H. Kozuka, T. Yoko, Mol. Cryst. Liquid Cryst. Sci. Technol., Sect. A 337 (1999) 217.
[19] M. Yoshimura, J. Mater. Res. 13 (1998) 796.
[20] Z. Wu, M. Yoshimura, Thin Solid Films 375 (2000) 46.
[21] D. Larcher, B. Gérand, J.-M. Tarascon, Int. J. Inorg. Mater. 2 (2000) 389.
[22] E. Vigil, L. Saadoun, R. Rodríguez-Clemente, J.A. Ayllón, X. Domènech, J. Mater. Sci. Lett. 18 (1999) 1067.
[23] E. Vigil, L. Saadoun, J.A. Ayllón, X. Domènech, I. Zumeta, R. Rodríguez-Clemente, Thin Solid Films 365 (2000) 12.
[24] E. Vigil, J.A. Ayllón, A.M. Peiró, R. Rodríguez-Clemente, X. Domènech, J. Peral, Langmuir 17 (2001) 891.
[25] A.M. Peiró, J. Peral, C. Domingo, X. Domènech, J.A. Ayllón, Chem. Mater 13 (2001) 2567.
[26] L. Saadoun, J.A. Ayllón, J. Jiménez-Becerril, J. Peral, X. Domènech, R. Rodríguez-Clemente, Mater. Res. Bull. 35 (2000) 325.
[27] J.A. Ayllón, A.M. Peiró, L. Saadoun, E. Vigil, X. Domènech, J. Peral, J. Mater. Chem. 10 (2000) 1911.
[28] O. Harizanov, A. Harizanova, Sol. Energy Mater. Sol. Cells 63 (2000) 185.
[29] N. Kaliwoh, J.-Y. Zhang, I.W. Boyed, Surf. Coat. Technol. 125 (2000) 424.
[30] A. Kay, M. Grätzel, Sol. Energy Mater. 44 (1996) 99.
[31] F. Izume, Bull. Chem. Soc. Jpn. 51 (1978) 1771.
[32] C. Minero, G. Mariella, V. Maurino, E. Pelizzetti, Langmuir 16 (2000) 2632.

5.4 Publicación 4

Electrochemically assisted deposition of titanium dioxide on aluminium cathodes

Ana M. Peiró,[a] Enric Brillas,[b] José Peral,[a] Xavier Domènech[a] and José Antonio Ayllón[a]

[a] Unitat de Química-Física, Departament de Química, Universitat Autònoma de Barcelona, 08193 Bellaterra, Barcelona, Spain

[b] Laboratori de Ciència i Tecnologia Electroquímica de Materials (LCTEM), Departament de Química Física, Facultat de Química, Universitat de Barcelona, Martí i Franquès 1, 08028 Barcelona, Spain

Journal of Materials Chemistry 12 (2002) 2769-2773

JOURNAL OF Materials CHEMISTRY

Electrochemically assisted deposition of titanium dioxide on aluminium cathodes

Ana M. Peiró,[a] Enric Brillas,[b] José Peral,[a] Xavier Domènech[a] and José A. Ayllón*[a]

[a]*Unitat de Química-Física, Departament de Química, Universitat Autònoma de Barcelona, 08193 Bellaterra, Spain*
[b]*Laboratori de Ciència i Tecnologia Electroquímica de Materials (LCTEM), Departament de Química Física, Facultat de Química, Universitat de Barcelona, Martí i Franquès 1, 08028 Barcelona, Spain*

Received 23rd April 2002, Accepted 6th June 2002
First published as an Advance Article on the web 25th July 2002

Adherent, uniform, and porous TiO_2 films have been obtained at ambient temperature by a novel electrochemical process involving the simultaneous cathodic electrodeposition of a Ti(IV)–peroxo complex and electrophoretic deposition of nanocrystalline TiO_2 particles on an Al cathode. Electrodepositions were performed using an electrolytic suspension containing a water-soluble titanium complex stabilized with a peroxo ligand and a commercial nanocrystalline TiO_2 powder (Degussa P25), and by applying a constant cell voltage between 2.0 and 4.5 V. The reduction process favours the decomposition of the soluble titanium complex to yield an amorphous TiO_2 precipitate on the cathode. This amorphous precipitate also acts as a binder to the nanocrystalline TiO_2 particles. The whole assembly shows photocatalytic activity for the degradation of salicylic acid without the need of thermal post-treatment.

1. Introduction

In recent years, there has been great interest in the preparation of TiO_2 films for their application in different technological fields, such as photocatalysis,[1–3] dye sensitized solar cells,[4–6] antireflective coatings,[7,8] and electrochromic devices.[9,10] A large number of techniques such as sol–gel,[11] CVD,[12] sputtering,[13] self-assembled monolayers,[14,15] liquid phase deposition,[16] atomic layer deposition,[17,18] and Langmuir–Blodgett[19] have been utilized for the fabrication of TiO_2 films. The development of new low-cost processes, which are of environmental interest, for the deposition of such films is of considerable interest. Electrochemical techniques using aqueous solutions provide an attractive approach to meeting these needs.

Some recent studies have shown that cathodic electrodeposition of TiO_2 films holds great promise for various applications.[20,21] This method is usually based on the electrochemical production of OH^- from the cathodic reduction of water or dissolved oxygen that promotes the precipitation on the cathodic substrate deposits of oxides and/or hydroxides of metallic ions or complexes contained in the electrolytic medium. However, although this process is performed at low temperatures, a post-annealing treatment is usually required to crystallize the amorphous deposit initially obtained. This technique has been successfully used to produce films of several oxides such as ZrO_2,[22] WO_3,[23] $ZrTiO_2$,[22] Nb_2O_5,[20] and ZnO,[21–24] as well as several composites, *e.g.* RuO_2–TiO_2 and Al_2O_3–TiO_2.[20] Several authors[9,20,25] have also reported the cathodic electrodeposition of TiO_2 films from soluble peroxo complexes in aqueous or aqueous alcohol solutions. The process is carried out in two-steps: in the first one, the soluble peroxo complexes are transformed by an electrogenerated base into insoluble species ($Ti(O_2)O_x{\cdot}H_2O$) which precipitate on the cathode, while in the second step this solid titania precursor, still containing the peroxo ligand and with an amorphous nature, is thermally decomposed. Crystallization to anatase is attained at 773 K.

Electrophoretic deposition is another electrochemical approach to the fabrication of ceramic films. This technique has allowed the preparation of films of several simple oxides such as alumina, zirconia,[26,27] TiO_2,[27–29] and composites (*e.g.* alumina–zirconia micro-laminate).[30,31] Although crystalline ceramic particles were employed in all the precursor suspensions, an annealing post-treatment at elevated temperature was necessary to sinterize the particles and produce well adhered dense films (*i.e.*, 573 K is the minimum temperature required to produce stable TiO_2 films on stainless steel[28]).

The aim of the present work is to combine both processes, cathodic electrodeposition and electrophoretic deposition, with the goal of obtaining photoactive TiO_2 films without the need of a thermal post-treatment. An aqueous electrolytic suspension for this novel electrochemical method has been chosen for environmental interest. The idea is that the electrodeposit formed from the soluble Ti(IV)–peroxo complex should act as a matrix that captures the nanocrystalline TiO_2 particles present in the electrolytic suspension. A high number of these nanoparticles should not be completely occluded by the matrix, their surface thus being accessible to yield photocatalytic processes. According to previous studies,[20] this matrix is expected to be composed of an insoluble polymeric titanium–peroxo complex. However, under the experimental conditions tested, the peroxo ligand decomposes, probably being cathodically reduced, and the matrix is thus transformed into conducting amorphous TiO_2. The photocatalytic activity of the deposited films has been tested in the degradation of an organic model compound such as salicylic acid (SA) in aqueous medium.

2. Experimental

2.1. Reagents

Titanium dioxide P25 (TiO_2 P25, 80% anatase, 20% rutile) was kindly supplied by Degussa. Tetraisopropyl orthotitanate (TIP) was from Fluka; nitric acid (HNO_3, 52.5%), absolute ethanol (EtOH) and concentrated hydrogen peroxide (H_2O_2, 30 wt% in H_2O) from Panreac, and salicylic acid from Merck. These chemicals were used without further purification. All solutions were prepared with high purity water produced by a Millipore Milli-Q system, with a conductivity lower than $6 \times 10^{-8}\,\Omega^{-1}\,cm^{-1}$ at 25 °C.

2.2. Preparation of the suspension for electrodeposition

Several procedures were attempted to prepare a stable electrolytic suspension, until an effective method was achieved: 0.375 g TiO_2 P25 (4.70 mmol) were ultrasonically dispersed in 25 mL of H_2O for 2 min and 360 μL of HNO_3 (4.71 mmol) were added afterwards. Then, 209 μL TIP (0.680 mmol) were dissolved in a mixture of 25 mL of EtOH and 70 μL of concentrated H_2O_2 (0.680 mmol). The solution of TIP was added dropwise to the suspension of TiO_2 P25 and the resulting suspension was homogenized by sonication for 10 min. The electrolytic medium thus obtained has a pH = 1.5, being stable at 298 K for more than 10 hours without separation of the TiO_2 powder.

2.3. Electrolytic cell and electrode cleaning

All electrodepositions were carried out in an open, one-compartment, cylindrical Pyrex cell of 120 cm^3 capacity having an external water jacket for temperature control. The cell contained the cathode centred between two parallel and equidistant anodes, with a gap of 1.4 cm. The dimensions of each electrode were 28 mm in length × 20 mm in width. Two nets (10 mm × 5 mm × 1 mm of mesh) of platinized titanium (with 2 μm of Pt thickness) supplied by Inagasa were used as Pt anodes. The cathode was an aluminium foil of 1 mm thickness, always being placed into the electrolytic suspension with an immersed surface area of 5.6 cm^2 each side. Before the electrodeposition process, both anodes were cleaned in a hot NaOH (0.25 M) solution for several minutes, and rinsed several times with bidistilled water and finally, with Milli-Q water. The cathode was polished with a sand bath, and consecutively sonicated with bidistilled water, ethanol, acetone and Milli-Q water. All electrolytic experiments were conducted in the potentiostatic mode using an Amel 2053 potentiostat-galvanostat. A constant cell voltage was applied ranging from 2.0 to 4.5 V. The electrolytic suspension was not stirred and its temperature was maintained at 298 K. After each electrodeposition trial, the coated aluminium foil was removed from the cell, rinsed several times with Milli-Q water to eliminate the residual components of the suspension and dried in an open atmosphere up to a constant weight. The weight of electrodeposited TiO_2 was then determined as the mass difference between the coated and uncoated cathode.

2.4. Characterization techniques

The surface morphology and thickness of the films were studied by scanning electron microscopy (SEM) with a Hitachi S-570 microscope. Samples were gold-covered for all SEM measurements. For thickness studies, samples were mounted onto a holder with an inclination of 45 degrees with respect to the electron beam. The crystalline phase of the films was analyzed by grazing angle X-ray diffraction (XRD) with a Siemens D-3400 diffractometer using Cu-K_α radiation ($\lambda = 0.154056$ Å) at 40 kV and 30 mA. The diffraction spectra were recorded at an incidence angle of 1.8 degrees over the degree range $15 < 2\theta < 65$.

2.5. Photocatalytic activity measurements

The degradation of SA under UV illumination was used as a test of the photocatalytic activity of the films. Experiments were carried out with films obtained at a cell voltage of 3.50 V after an electrodeposition time of 90 min. The TiO_2 film was placed in a 100 mL aqueous solution of 0.25 mmol L^{-1} SA filling a thermostated cylindrical Pyrex cell, in which the temperature was kept at 298 K. The solution was maintained under stirring with a magnetic bar throughout the experiment, and air was bubbled through it. A 125 W Philips HPK medium-pressure mercury vapour lamp was used as light source. The TiO_2-covered aluminium foil was placed parallel to the light direction in the middle of the lamp's beam so that both faces were illuminated. The SA concentration was followed by measuring the absorbance of aliquots with a Philips PU 8620 UV/VIS/NIR spectrophotometer at a wavelength of 296 nm (the maximum of the absorption peak of SA). Quartz cuvettes of 1 cm optical path length were used.

3. Results and discussion

3.1. Preparation and composition of TiO_2 films

The electrolytic suspension used for electrodeposition contains nanocrystalline TiO_2 particles at pH = 1.5. This pH value is well below the pH of zero charge of TiO_2 (pH = 6.2) and thus, the particles are expected to be positively charged by adsorbed protons. On the other hand, when TIP is dissolved in absolute EtOH and H_2O_2 is added, a yellow solution is obtained due to the formation of peroxotitanium complexes, which prevent the condensation of Ti cations. In the electrolytic suspension of pH 1.5, these complexes are also positively charged and their main components are dinuclear species.[30] The existence of positive charges also impedes the adsorption of such titanium soluble species on the TiO_2 electrodeposits.

Electrolyses were carried out by applying a constant cell voltage higher than 2.0 V between the electrodes, trying to induce two parallel electrodeposition processes (cathodic and electrophoretic) on the Al cathode. At these high cell voltages, both processes also compete with the fast electrogeneration of OH^- from the reduction of dissolved oxygen, and/or the depletion of protons by their reduction to hydrogen gas. Thus, when the positively charged peroxotitanium complex reaches the vicinity of the cathode, where the pH is basic due to the presence of electrogenerated OH^- ions, it reacts with the precipitation of an insoluble peroxotitanium hydrate, $TiO_3(H_2O)_x$ ($1 < x < 2$).[20,22,32] In addition, the positively charged TiO_2 nanoparticles move electrophoretically toward the cathode, being codeposited with the above mentioned peroxotitanium hydrate. Electrodeposited TiO_2 films thus obtained were white, as expected when no peroxo species are present, at least not in any significant proportion. This point was confirmed by the high stability of the films when treated with strong acidic solution (HNO_3 or HCl) at room temperature. It can then be inferred that during the electrolytic process, the insoluble $TiO_3(H_2O)_x$ decomposes, probably by cathodic reduction, and for this reason it is not present in the final TiO_2 electrodeposit. It is noteworthy that the yellow colour of the suspension faded away as the electrodeposition process took place, while the pH of the solution remained practically constant throughout the electrolysis (near 1.5), indicating that all the soluble peroxo species are consumed in the process.

The composition of the deposits was characterized using XRD. Fig. 1 shows the XRD patterns of a TiO_2 film electrodeposited at a constant cell voltage of 3.50 V for 30 min. According to the JCPDS reference data, the main diffraction lines were identified as those corresponding to TiO_2 anatase (A), TiO_2 rutile (R) and aluminium (Al); very small peaks due to Al_2O_3 were also observed. Anatase and rutile phases are present in the films in the same ratio as in TiO_2 P25, confirming that the nanocrystalline TiO_2 powder has been incorporated into the films. These results rule out the formation of crystalline TiO_2 from the possible cathodic reduction of insoluble $TiO_3(H_2O)_x$. Due to the low temperature of the process, the titania formed in the reduction of the soluble peroxotitanium precursor (which accounts for 14% of the titanium contained in the electrolytic suspension) should be amorphous, and therefore, will not exhibit any diffraction peak.

Efforts were then devoted to show the presence of amorphous titania in the films produced by the proposed

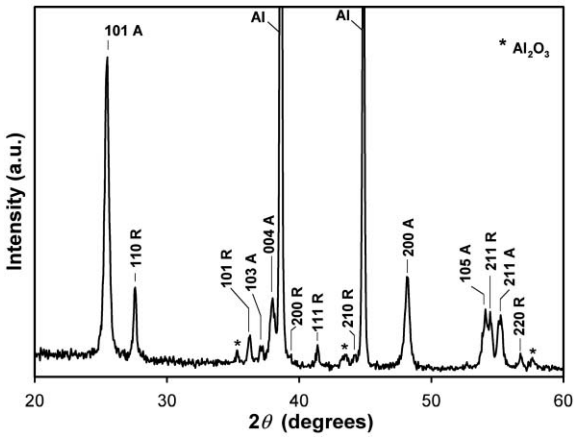

Fig. 1 Grazing incidence X-ray diffractogram corresponding to a TiO_2 film electrodeposited onto an aluminium substrate. The main diffraction peaks correspond to anatase (A), rutile (R), and aluminium substrate (Al). Applied cell voltage 3.50 V. Electrodeposition time 30 min. Temperature 298 K.

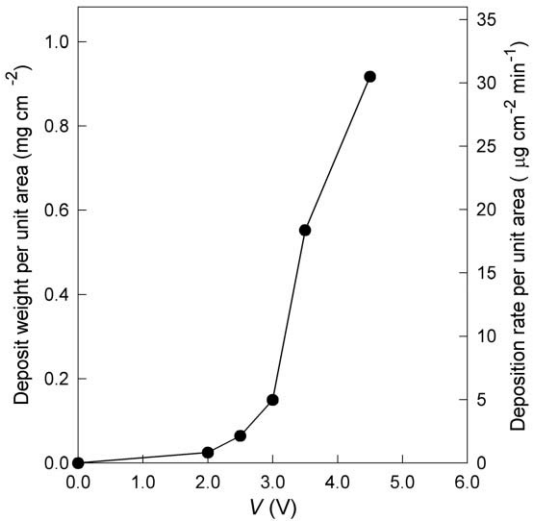

Fig. 2 Variation of the weight of electrodeposited TiO_2 or its electrodeposition rate per unit area with applied cell voltage over 30 min. Temperature 298 K.

electrochemical method. Initial confirmation was made by treating the electrodeposits with a solution containing H_2O_2 and strong acid. In these treatments, yellow solutions were obtained leading to a partial detachment of films, which can be ascribed to the partial solubilization of amorphous titania contained in them. In addition, several electrolyses were also performed without the soluble peroxotitanium precursor in the electrolytic bath, but no films grew on the cathode surface. This behaviour allows us to establish that the amorphous titania produced from the insoluble $TiO_3(H_2O)_x$ acts as a binder of the codeposited nanocrystalline TiO_2 particles.

3.2. Electrodeposition behavior

Different electrolytic conditions were tested in an attempt to obtain TiO_2 electrodeposits. The use of a constant current led to a progressive increase in cell voltage producing deposits of very low adherence. The potentiostatic method was preferred because adherent, uniform, and white deposits grew by applying a constant cell voltage ranging from 2.0 to 4.5 V for times of up to 90 min. However, lower cell voltages did not yield films, probably because of the low electrogeneration rate of OH^- that prevents cathodic electrodeposition of the soluble titanium complex, whereas cell voltages higher than 4.5 V caused a fast stripping of deposits.

Fig. 2 shows a non-linear behaviour of the weight of deposited material at the cathode per unit area, or the rate of electrodeposition per unit area, with increasing voltage for a fixed electrodeposition time of 30 min. As can be seen, the electrodeposition rate is moderately low below 3.0 V, but rapidly increases to *ca.* 30 μg cm^{-2} min^{-1} at 4.50 V. Fig. 3 presents the change of deposit weight per unit area *vs.* the electrodeposition time for a constant cell voltage of 3.50 V. Faradaic behaviour can be observed until 60 min, for which an average electrodeposition rate of *ca.* 17 μg cm^{-2} min^{-1} is obtained. However, at 90 min, the deposit weight is lower than expected, while longer times promote a partial film stripping.

The data in Figs. 2 and 3 allow us to conclude that the amount of electrodeposited TiO_2 can be controlled either by adjusting the applied cell voltage at a fixed electrodeposition time or by varying such time at a given cell voltage, always limiting the cell voltage to between 2.0 and 4.5 V and the electrodeposition time to 90 min. Under these conditions, a relatively high cathodic current density (j_{cat}) is always found. This can be observed in Fig. 4, where the time dependence of j_{cat} for a cell voltage of 3.50 V is depicted. Similar j_{cat}–t curves were obtained for other experiments performed under the

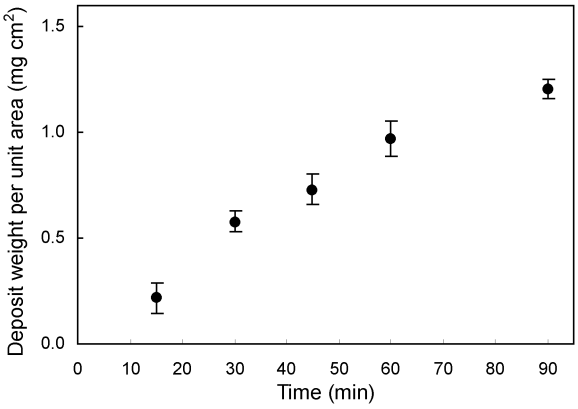

Fig. 3 Dependence of the weight of electrodeposited TiO_2 on electrodeposition time for a constant cell voltage of 3.50 V. Temperature 298 K.

conditions shown in Fig. 3. In all cases, the initial cathodic current density drops rapidly reaching a value of *ca.* 5.2 mA cm^{-2} after the first minute, when a thin film already covers the immersed cathode surface. The subsequent slight, but gradual, decay of j_{cat} with time can be ascribed to the increasing electrical resistance of the thickening coating.

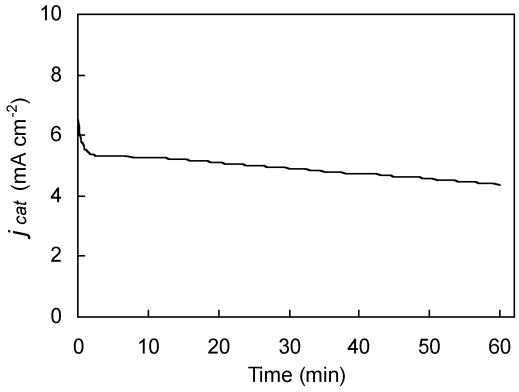

Fig. 4 Cathodic current density *vs.* electrodeposition time on applying a constant cell voltage of 3.50 V. Temperature 298 K.

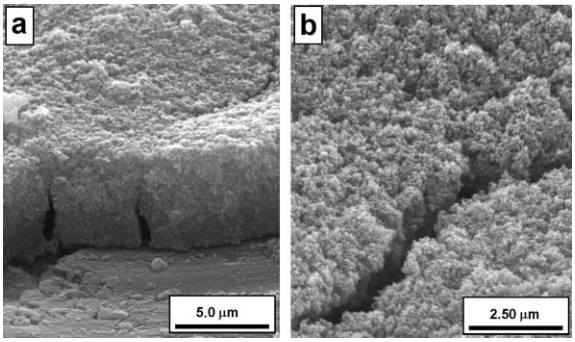

Fig. 5 SEM images taken at 45 degrees for a TiO_2 film electrodeposited for 90 min on Al: (a) cross-section of a step; (b) detail showing the porous texture of the film. Applied cell voltage 3.50 V. Temperature 298 K.

3.3. Thickness and morphology of TiO_2 electrodeposits

The thickness of the films was measured using both SEM and weight methods. As an example, two SEM cross-sections of the TiO_2 electrodeposits obtained after different times are depicted in Fig. 5. Although no regular films can be observed, SEM measurements allowed us to measure an electrodeposition rate of approximately 0.15 μm min^{-1} under the conditions given in Fig. 3 for a cell voltage of 3.50 V. On the other hand, the average thickness of these deposits was also calculated from its weight, once the area of the covered substrate was known, and by assuming that the films are compact (weight method). The density of electrodeposited TiO_2 required for this calculation was assumed to be the same as that of TiO_2 P25 supplied by Degussa,[33] *i.e.* 3.7 g cm^{-3}, because of the similar structure of both materials, as above pointed out. The thickness of the films were estimated by this method to be between 2 and 4.5 times lower than those experimentally obtained by SEM measurements. This difference clearly indicates that the films are porous. In fact, the high porosity of the films can be readily observed in the SEM image of Fig. 5(b).

The surface morphology of TiO_2 electrodeposited films on Al was also studied by SEM. As it is shown in Figs. 6(b)–6(e), all deposits obtained with a cell voltage of 3.50 V exhibit significant cracking, which may be related to the drying process or be induced by the Al substrate morphology (see Fig. 6(a)). The Al substrate presents a rough surface that can affect not only the morphology of the deposit but its adhesion, as well. To clarify this point, supplementary electrodepositions were performed under the same conditions using Al cathodes, polished using a combination of a sand paper and diamond grit polishing paste of 6 and 1 μm, respectively. For these experiments, less TiO_2 was electrodeposited than experiments performed with rougher Al surfaces, but similar cracking was observed in both cases. These results allow us to conclude that cracking occurs during the drying process.

3.4. Photocatalytic activity of electrodeposited TiO_2 films

The photocatalytic activity of the electrodeposited TiO_2 films was studied by testing their ability to degrade a 100 mL solution of 0.25 mmol L^{-1} salicylic acid. This acid has been chosen as a model compound to test the activity of TiO_2 in a large number of papers,[34–38] not only because it is a common pollutant in industrial waste waters (paper milling, cosmetic industries, landfill leachate),[39] but also because its molecular structure is similar to many other toxic compounds. Comparative trials were carried out using the SA solution with and without an Al substrate coated with a TiO_2 film deposited at 3.50 V for 90 min. In each case, treatment in the dark for 120 min was performed initially to evaluate possible adsorption phenomena or instability of the system, followed by exposure to UV light for 150 min. The relative concentration of SA,

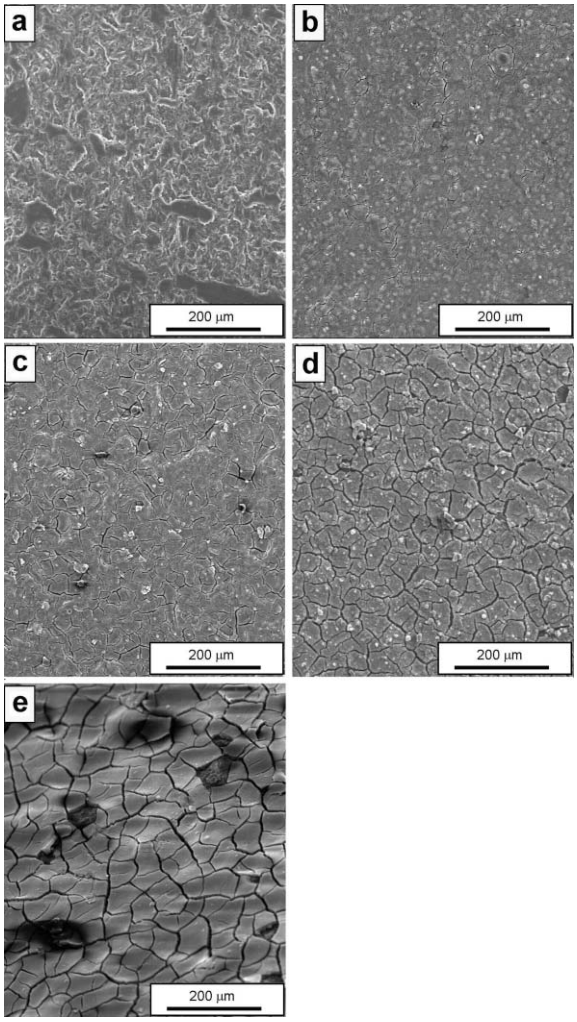

Fig. 6 SEM micrographs showing the surface morphology of (a) Al substrate and of TiO_2 films electrodeposited on Al cathodes after different periods of time: (b) 30, (c) 45, (d) 60, and (e) 90 min. Applied cell voltage 3.50 V. Temperature 298 K.

determined as the ratio between the absorbance at time t and the initial absorbance, both at 296 nm, is depicted in Fig. 7. Reproducible results were obtained for different films prepared and used under the same experimental conditions. From the data in Fig. 7, it can be inferred that there is no loss of the organic compound by volatilization or air stripping, since in the dark and without TiO_2, no change in the SA concentration

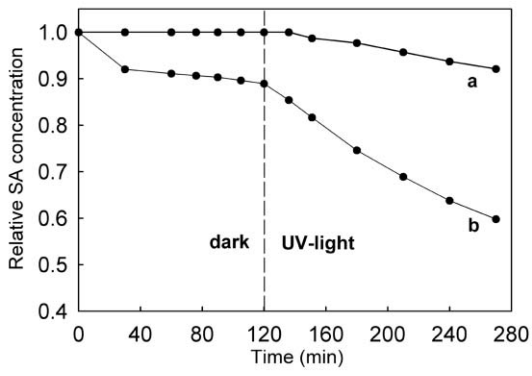

Fig. 7 Time course of the relative concentration of SA in aqueous solution: (a) in the dark without TiO_2, followed by UV illumination; and (b) in the dark with a TiO_2 film, followed by UV illumination. Experimental conditions: $[SA]_0$ = 0.25 mmol L^{-1}, pH_0 = 3.0, air bubbling, irradiation with a 125 W medium pressure Hg vapour lamp, and temperature 298 K. The TiO_2 electrodeposit was prepared at a constant cell voltage of 3.50 V for 90 min.

was noticed. In the dark and in the presence of a TiO_2 film, a fast decrease in the concentration of salicylic acid, stabilized to *ca.* 10%, takes place as a consequence of its adsorption on the catalyst surface. As can be seen in Fig. 7(b), illumination of the solution in the presence of a TiO_2 film leads to a significant reduction in the SA concentration: about 30% in 150 min. The percentage of SA degraded by direct photolysis in the same time (see Fig. 7(a)) is less than 5%, a negligible value compared to the removal observed with a TiO_2 film. Considering that amorphous titania is not photoactive,[40] the photoactivity detected for the electrodeposited films should be ascribed to the existence of nanocrystalline TiO_2 at their surface. This fact indicates that during electrodeposition TiO_2 particles are not completely occluded by the amorphous TiO_2 binder.

Conclusions

It has been demonstrated that adherent, uniform, and porous TiO_2 films can be electrodeposited on aluminium at ambient temperature with a novel electrochemical method that involves the simultaneous cathodic and electrophoretic deposition of two titania species present in a stable aqueous suspension. This process is possible using a constant cell voltage between 2.0 and 4.5 V, conditions under which OH^- is also electrogenerated in the vicinity of the cathode. Thus, electrophoretically deposited nanocrystalline TiO_2 particles can be immobilised onto the metal substrate by an amorphous TiO_2 matrix produced from the cathodic electrodeposition of a soluble peroxotitanium precursor. This last process involves the initial precipitation of a peroxotitanium hydrate by reaction of this precursor with electrogenerated OH^-, followed by its decomposition, probably by cathodic reduction, to the final conducting amorphous titania. The film thickness can be controlled either by the cell voltage applied and/or by its electrodeposition time up to 90 min. The films show photocatalytic activity without the need of thermal post-treatment, indicating that their nanocrystalline TiO_2 particles are not completely occluded by the amorphous titania matrix.

References

1 R. L. Pozzo, M. A. Baltanás and A. E. Cassano, *Catal. Today*, 1997, **39**, 219–231.
2 Y. Jiaguo, Z. Xiujian and X. Qingnan, *Mater. Chem. Phys.*, 2001, **69**, 25–29.
3 A. P. Xagas, E. Androulaki, A. Hiskia and P. Falaras, *Thin Solid Films*, 1999, **357**, 173–178.
4 Y. Li, J. Hagen, W. Schaffrath, P. Otschik and D. Haarer, *Sol. Energy Mater. Sol. Cells*, 1999, **56**, 167–174.
5 C. J. Barbé, F. Arendse, P. Comte, M. Jirousek, F. Lenzmann, V. Shklover and M. Grätzel, *J. Am. Ceram. Soc.*, 1997, **80**, 3157–3171.
6 G. Phani, G. Tulloch, D. Vittorio and I. Skryabin, *Renewable Energy*, 2001, **22**, 303–309.
7 G. San Vicente, A. Morales and M. T. Gutierrez, *Thin Solid Films*, 2001, **391**, 133–137.
8 L. M. Doeswijk, H. H. C. de Moor, D. H. A. Blank and H. Rogalla, *Appl. Phys. A: Solid Surf.*, 1999, **69 (Suppl)**, S409–S411.
9 C. Natarajan and G. J. Nogami, *J. Electrochem. Soc.*, 1996, **143**, 1547–1550.
10 S. K. Poznyak, V. V. Sviridov, A. I. Kulak and M. P. Samtsov, *J. Electroanal. Chem.*, 1992, **340**, 73–97.
11 Y. Zhu, L. Zhang, L. Wang, Y. Fu and L. Cao, *J. Mater. Chem*, **11**, 1864–68.
12 B.-C. Kang, S.-B. Lee and J.-H. Boo, *Surf. Coat. Technol.*, 2000, **131**, 88–92.
13 D. Mardare, M. Tasca, M. Delibas and G. I. Rusu, *Appl. Surf. Sci.*, 2000, **156**, 200–206.
14 Y. Masuda, T. Sugiyama, H. Lin, W. S. Seo and K. Koumoto, *Thin Solid Films*, 2001, **382**, 153–157.
15 H. Shin, R. J. Collins, M. R. De Guire, A. H. Heuer and C. N. Sukenik, *J. Mater. Res.*, 1995, **10**, 692–698.
16 H. Kishimoto, K. Takahama, N. Hashimoto, Y. Aoi and S. Deki, *J. Mater. Chem.*, 1998, **8**, 2019–2024.
17 M. Ritala, M. Leskela, L. Niinisto and P. Haussalo, *Chem. Mater.*, 1993, **5**, 1174–1781.
18 M. Ritala, M. Leskela, E. Nykaenen, P. Soininen and L. Niinisto, *Thin Solid Films*, 1993, **225**, 288–295.
19 J. Jin, L. S. Li, Y. Li, X. Chen, L. Jiang, Y. Y. Zhao and T.-T. Li, *Thin Solid Films*, 2000, **379**, 218–223.
20 I. Zhitomirsky, *J. Eur. Ceram. Soc.*, 1999, **19**, 2581–2587.
21 S. Peulon and D. J. Lincot, *J. Electrochem. Soc.*, 1998, **145**, 864–874.
22 I. Zhitomirsky and L. Gal-Or, *J. Eur. Ceram. Soc.*, 1996, **16**, 819–824.
23 E. A. Meulenkamp, *J. Electrochem. Soc.*, 1997, **144**, 1664–1671.
24 M. Izaki and T. Omi, *J. Electrochem. Soc.*, 1997, **144**, 1949–1952.
25 I. Zhitomirsky, *Nanostruct. Mater.*, 1997, **8**, 521–528.
26 T. Uchikoshi, K. Ozawa, B. D. Hatton and Y. Sakka, *J. Mater. Res.*, 2001, **16**, 321–324.
27 I. Koengeter, I. Wuehrl, U. Eisele, R. Drumm, S. Knoll R. Nonninger and H. Schmidt, *Ger. P.*, 2000, 19919818.
28 J. A. Byrne, B. R. Eggins, N. M. D. Brown, B. Mckinney and M. Rouse, *Appl. Catal. B: Environ.*, 1998, **17**, 25–36.
29 D. Matthews, A. Kay and M. Graetzel, *Aust. J. Chem.*, 1994, **47**, 1869–1877.
30 R. Fischer, E. Fischer, G. de Portu and E. Roncari, *J. Mater. Sci. Lett.*, 1995, **14**, 25–27.
31 P. S. Nicholson, P. Sarkar and X. Haung, *J. Mater. Sci.*, 1999, **28**, 6274–6278.
32 J. Mühlenbach, K. Müller and G. Schwarzenbach, *Inorg. Chem.*, 1970, **9**, 2381–2390.
33 M. Ettingler, *Degussa Technical Bulletin Pigments*, vol. 56, Degussa AG, Frankfurt, Germany, 1993.
34 A. E. Regazzoni, P. Mandelbaum, M. Matsuyoshi, S. Schiller, S. A. Bilmes and M. A. Blesa, *Langmuir*, 1998, **14**, 868–874.
35 V. Sukharev, A. Wold, Y.-M. Gao and K. Dwight, *J. Solid State Chem.*, 1999, **119**, 339–343.
36 G. Li Puma and P. L. Yue, *Chem. Eng. Sci.*, 1998, **53**, 3007–3021.
37 S. Tunesi and M. Anderson, *J. Phys. Chem.*, 1991, **95**, 3399–3405.
38 K. Katrochrilova, I. Hoskovcová, J. Jirkovsky, J. Klíma and J. Ludvik, *Electrochim. Acta*, 1995, **40**, 2603–2609.
39 A. Mills, C. E. Holland, R. H. Davies and D. J. Worsley, *Photochem. Photobiol. A.: Chem.*, 1994, **83**, 257–263.
40 B. Ohtani, Y. Ogawa and S.-i. Nishimoto, *J. Phys. Chem. B*, 1997, **101**, 3746–3752.